UNIVERSITY OF CALIFORNIA, BERKELEY

BERKELEY • DAVIS • IRVINE • LOS ANGELES • RIVERSIDE • SAN DIEGO • SAN FRANCISCO

SANTA BARBARA • SANTA CRUZ

DEPARTMENT OF PHYSICS

BERKELEY, CALIFORNIA 94720

1

November 14, 1990

Scientific Officer Code: 1112LO
Herschel S. Pilloff — 696-4223
Office of Naval Research code 1112LO
800 North Quincy Street
Arlington, Virginia 22217-5000

Reference N00014-90-J-1475-Clauser
UCB Account No. 1-444010-23069

Enclosed you will find the Third Quarterly Report on Professor John F. Clauser's project entitled, "Neutral Atom Matter-Wave Interferometry".

Sincerely yours,

Mary P. Gilmore
Accounting Office Supervisor
Physics Department
(415) 642-2943

cc: Administrative Grants Officer: Code N 63373
Director, Naval Research Lab: Code 2627
Defense Technical Information Center
Norma Morales, Financial & Business Services

Quarterly Report for ONR Grant N00014-90-J-1475.
Neutral Atom deBroglie-Wave Interferometry
Year 1, Quarter 3, August - October 1990
Principal Investigator: John F. Clauser

Vacuum System & Thermal Beam Generator:

The oven heater circuit was split into two separate circuits to reduce its thermal gradients gradient. New power and temperature monitor circuits were completed, installed and tested.

Vibration Isolation System:

Three generations of pneumatic support pistons were fabricated, installed, and tested, with each an improvement of the previous. Final system test currently awaits the next pump down. A summary report *Matter-Wave Interferometry Vibration Isolation* (requested by ONR) was submitted 3 October.

Laser Systems:

Diode lasers have been successfully temperature tuned using a single - stage thermoelectric cooler. To narrow the laser line-width, a cavity consisting of the laser itself on one end and a diffraction reflection grating on the other (design patterned after that by Wieman and Holberg) has been built and tested. It appears to perform exactly as advertised with a continuous tuning range of about 5nm and a measured line width of about 100kHz. In addition, we have been able to modulate the beam up to about 80 MHz. At higher frequency, RF pickup and diminishing photodiode frequency response prevented confirmation of the modulation, which we believe is still present. We are nearly ready to test this in combination with two - stage thermoelectric cooling. Initial tuning checks will be with a potassium hollow cathode lamp via the optogalvanic effect. Following these tests, we will mount it on the vacuum chamber as a probe laser for the beam fluorescence experiments.

Fluorescence Beam-Velocity Monitor:

Construction is nearly complete of optics and photomultiplier systems for monitoring the fluorescence produced by the

interaction of the probe laser with the potassium beam, as well as the probe laser transport optics and mountings. Experiments to measure the thermal velocity distribution from our oven and to detect the potassium hyperfine structure will commence shortly.

Matter-Wave Interferometry:

A report *Application of Fourier - Fresnel Imaging to Neutral - Atom Interferometry* (requested by ONR) was submitted 3 October.

Reports:

Three reports requested by ONR have been submitted:

1. *Application of Fourier - Fresnel Imaging to Neutral*,
2. *Matter-Wave Interferometry Vibration Isolation - Atom Interferometry*)
3. *Response to summary Questionnaire.*

Matter-Wave Interferometry Vibration Isolation

John F. Clauser
Physics Dept., Univ. of Calif. - Berkeley
3 October, 1990

In this note we provide a brief summary of vibration isolation techniques and their application to our neutral atom interferometry experiments at the UC Berkeley Physics Department. Naturally, the difficulty in achieving acceptable vibration isolation for any given experiment depends largely upon the noise background of the laboratory, the noise generated by the experimental apparatus itself, as well as the tolerable noise sensitivity of the experiment. Since neutral atom interferometers may be configured to act as ultra-sensitive inertial sensors, their vibrational noise sensitivity is inherently high.

1. What constitutes signal & what constitutes noise?

The initial experiments at UCB are to simply demonstrate neutral atom interference. For these experiments any deviations from an inertial reference frame for the apparatus represent a potential noise source. Even the quasi-constant earth's gravitational field and rotation can be considered as very low frequency noise components, although subsequent experiments will consider these as known test signal's to be measured.

2. Vibration sensitivity of neutral atom interferometry experiments:

Our proposed neutral atom interferometer includes the following components: (a) a source of slow, cold atoms, (b) a sequence of transmission diffraction gratings, and (c) an atomic particle detector. The interferometer's parameters were selected to de-emphasize its inertial sensitivity and thereby assure success of the initial experiments. Nonetheless, it is still quite sensitive to inertial forces, such as those caused by vibrationally induced acceleration. Its sensitive axis is in a direction perpendicular to the source-detector axis and perpendicular to the grating slits' long direction. It has negligible sensitivity to inertial forces acting perpendicular to

its sensitive axis.

Unfortunately, for any experiment in a terrestrial laboratory, gravity cannot be eliminated. Thus, it is worthwhile to orient the apparatus so that gravity is perpendicular to the sensitive axis. In our case, this is done by having the beam propagate vertically. An advantage of this orientation is that the axial alignment remains independent of atomic velocity.

The purpose of our initial experiments is simply to detect interference fringes. Hence, one desires that the peak-to-peak worst-case vibration noise be limited to provide less than one fringe shift in whatever observation period is necessary for positive identification and measurement of the atomic fringe structure. In simplest terms, this requirement translates to the requirement that the worst-case peak-to-peak vibration amplitude (relative to an inertial frame) of any grating be much less than one slit width of that grating. If phase sensitive detection is employed, this limiting amplitude constrains the apparatus allowed vibration only over the bandwidth of the fringe detector, which, in turn, can be made quite narrow, and furthermore, can be centered at a vibrationally quiet portion of the spectrum. With phase sensitive detection the above constraint may be relaxed at frequencies outside this bandwidth.

Why does the slit width represent a limiting amplitude for vibrations? Indeed, for periodic vibrations of constant amplitude the amplitude of the resulting acceleration scales with the square of the vibration frequency. Thus, one might expect that the interferometer fringe shift (proportional to linear acceleration) will scale similarly. Fortunately, this is not the case for periodic accelerations with frequencies higher than the inverse transit time of atoms through the interferometer. For such frequencies the accelerational sensitivity decreases inversely with frequency squared, so that the limiting spatial amplitude for vibrations is still just the slit width.

To visualize this dependence, consider in an inertial frame waves passing through a set of vibrating gratings. The diffraction pattern at the final grating (and the Moiré pattern formed by this pattern and the final grating) is given by the Kirchoff diffraction integral over possible paths (in the inertial frame)

from the source, through all open slits to the final grating. The possible paths traversed by any given wavefront constitute those open at the time of its passage. Thus, even though a grating may rapidly vibrate during the passage of a wavefront through a slit, so long as the majority of paths offered by open slits remain open for the passage of subsequent wavefronts, then the Kirchoff diffraction integral will be negligibly altered. That is, as long as a only negligible fraction of each slits' open cross-section is affected by the vibration, the diffraction pattern will be maintained. This will be true as long as the worst-case wiggling of the edges of these paths remains small with respect to a slit width.

Our initial experiments anticipate the use of about 1/2 to 1 micron slits, a path length of 0.92m, and a lowest velocity (with correspondingly highest accelerational sensitivity) of 5 - 10 m/sec. The worst case vibrational noise occurs at a frequency of 1/τ(transit), or 5 - 10 Hz. Since externally produced high frequency (>> 1Hz) vibrations are comparatively easy to isolate from the apparatus but the support structure must pass zero frequency, it is the lowest frequency components (0.1 - 5 Hz) that are potentially the most troublesome.

Another potential source of noise is that due to structural flexure within the apparatus. Such flexure can allow one grating to vibrate relative to another one and thereby couple additional noise into the system. Unless sufficient damping is provided, apparatus generated noise may be trapped within the isolated apparatus. Structural flexure resonances can then cause amplification of these vibrations and significant relative motion of the gratings will produce additional noise. Fortunately, relative motion of the gratings is detectable with *in-situ* optical interferometry and, if found present, can be remedied by eliminating resonances and/or introduction of additional damping.

3. Noise sources in Room 318 LeConte, UCB Physics Dept.:

Potential external sources of vibration include various forms of cultural noise (e.g. hallway traffic), building plant noise (typically rotating machinery), seismic activity, etc. Its magnitude depends on the laboratory construction, location within

the building and the time of day. On the third floor of LeConte Hall, all of these sources have been measured at various times, with frequency spectra in the range of a few Hz to a few 10's of Hz. Vibrations of the same order of magnitude are measurable in vertical and horizontal directions, as well as in rolling motions of the floor. Typical vibration amplitudes in Room 318 are of order 1-4 microns. Although the floor's rolling motion is large, suspending the entire apparatus on a two-axis knife-edge bearing prevents coupling this motion into the rotational modes of the apparatus. With significant apparatus height above the floor, the rolling motion produces an amplified horizontal motion of the apparatus. The rolling motion thus requires significant horizontal isolation of the apparatus center of gravity, provided by a flexible leg support structure and damped pneumatic pistons. Isolation ratios of 10 to 100 from floor vibrations will suffice, even for experiments not using phase sensitive detection. Phase sensitive detection can further reduce vibrational noise to total insignificance.

4. Techniques:

There are two basic popular methods for isolation of scientific apparatus: active and passive. Passive (conventional) isolation systems are based on the low-pass filter action of a spring-mass-dashpot linear system. Higher isolation using the same principles is available by cascading such filters (as is commonly done in gravitational wave detection experiments). The basic physics of such isolation is given in the attached excerpt from a Newport Research Corporation catalog. Passive isolation systems and components are commercially available for supporting large apparatus. Unfortunately, such commercial components are awkward to use with an apparatus with significant vertical height (such as ours).

Active isolation systems sense vibrational acceleration of the apparatus with an accelerometer and apply a corrective force via an electronic feedback system. Such systems are complex and costly. Commercial active systems are presently available only for small apparatus.

The present system at UCB is passive and successfully

isolates building noise to the required degree not to require phase sensitive detection. Apparatus self-noise at present dominates. It is evidently due to vibrations caused by boiling liquids in the diffusion pumps and liquid nitrogen traps. Significant noise is found to exist in the isolator normal modes only when the pumps are on and the traps are full. Experiments currently underway will determine whether this noise can be brought to an acceptable level by damping improvements. If not, these pumps and traps may be replaced with sorption roughing pumps and ion high-vacuum pumps.

Fundamentals of Vibration

Many problems of vibration are caused by structural resonances of the measurement apparatus – for example the table on which an optical interferometry experiment is performed. Vibration and vibration isolation are both intimately connected with the phenomenon of resonance which is illustrated in this section by the two basic models below.

Model I: The Simple Harmonic Oscillator

The simple harmonic oscillator consists of a rigid mass M connected to an ideal linear spring as shown in Figure A.

Fig. A: Simple harmonic oscillator consisting of a mass and a spring.

The spring has a static compliance C such that the change in length of the spring Δx that occurs in response to a force F is

$$\Delta x = C F$$

Note that the compliance C is the inverse of the spring stiffness (commonly denoted by k) since $C = 1/k$.

If the spring-mass system is driven by a sinusoidal displacement with frequency ω and peak amplitude $|x_0|$, it will produce a sinusoidal displacement of the mass M with peak amplitude $|x|$ at the same frequency ω. The steady-state ratio of the amplitude of the mass motion $|x|$ to the spring end motion $|x_0|$ is called the transmissibility T and is given by

$$T = \left| \frac{x}{x_0} \right| = \frac{1}{\left| 1 - \omega^2 / \omega_n^2 \right|}$$

where ω_n is the resonance or natural frequency of the system given by

$$\omega_n = \frac{1}{\sqrt{CM}}$$

Note that the natural frequency of the system ω_n is determined solely by the mass and the spring compliance. It decreases for a larger mass or a more compliant (softer) spring. The transmissibility T of the system is plotted as a function of the frequency ratio ω/ω_n on a log-log plot in Figure B.

The three characteristic features of this system are:

1) For $\omega \ll \omega_n$, well below the resonance frequency, the transmissibility T = 1 so the motion of the mass is the same as the motion of the other end of the spring.

2) For $\omega = \omega_n$, near resonance, the motion of the spring end is amplified and the motion of the mass $|x|$ is greater than that of $|x_0|$. For an undamped system, the motion of the mass becomes theoretically infinite for $\omega = \omega_n$.

3) For $\omega \gg \omega_n$, the resulting displacement $|x|$ decreases in proportion to $1/\omega^2$. In this case the displacement $|x_0|$ applied to the system is not transmitted to the mass. In other words, the spring acts like an isolator.

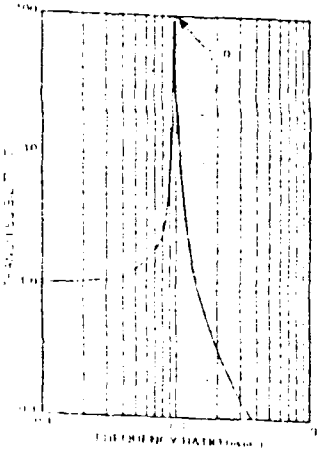

Fig. B: Transmissibility of a simple harmonic oscillator.

Model II: The Damped Simple Harmonic Oscillator

In the first model we considered an undamped system in which there is no mechanism to dissipate mechanical energy from the mass-spring system. Damping refers to a mechanism that removes the mechanical energy from the system – very often as heat. A damped simple harmonic oscillator is shown schematically in Figure C.

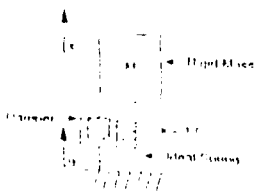

Fig. C: Damped simple harmonic oscillator consisting of a mass, a spring and a damper.

A rigidly connected damper is expressed mathematically by adding a damping term proportional to the velocity of the mass and to the differential equation describing the motion. For an external force that results in a displacement amplitude $|x_0|$ of the end of the spring as in Model I, the transmissibility T of the damped system becomes:

$$T = \left| \frac{x}{x_0} \right| = \sqrt{\frac{1 + (2\zeta\omega/\omega_n)^2}{\left[1 - (\omega/\omega_n)^2\right]^2 + (2\zeta\omega/\omega_n)^2}}$$

where ζ is a dimensionless damping coefficient given by:

$$\zeta = \frac{b}{2\sqrt{CM}}$$

A plot of the transmissibility T is shown in Figure D for various values of the damping coefficient ζ. In the limit where ζ approaches zero, the curve becomes exactly the same as in Model I, that is, there is infinite amplification at the resonance frequency ω_n. As the damping increases, the amplitude at resonance decreases. However, the "roll-off" at *higher* frequencies decreases (i.e. the transmissibility declines more slowly as damping increases). For $\omega/\omega_n \gg 1/2\zeta$, note that the motion of $|x|$ is proportional to $1/\omega$ as compared to Model I where at high frequencies the motion of $|x|$ decreases as $1/\omega^2$.

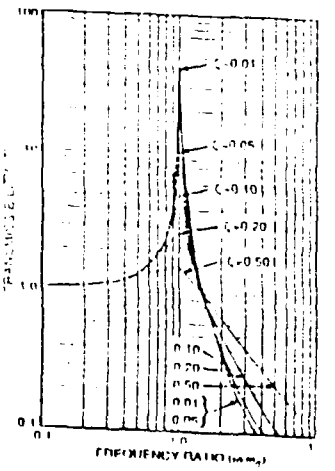

Fig. D: Transmissibility of a damped oscillator system with various values of damping coefficient (ζ).

Pneumatic isolators are one of the best methods of vibration isolation for critical applications. When properly designed and carefully constructed, their performance combines the "fast roll off" of the simple harmonic oscillator at vibration frequencies above resonance with the "low amplification at reso-

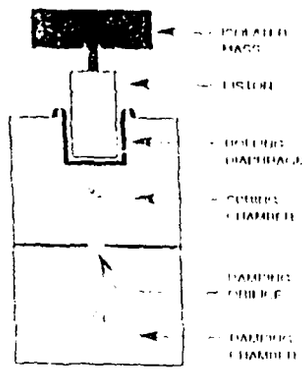

Fig 1 Pneumatic isolation with damping

nance" of the damped harmonic oscillator near resonance.

The basic design for a pneumatic isolator with damping is shown in Figure 1. The isolated mass M (for example, an optical table or precision instrument such as a microscope) is supported by a piston which rests on a flexible rolling diaphragm. The diaphragm separates the piston from the top section of the air chamber called the "spring chamber". In damped systems, air can flow between the spring chamber and a secondary chamber, called the "damping chamber" through a flow restrictor, usually a small orifice. As air flows through the orifice, energy is dissipated, reducing the amplification of the isolator at resonance. The theoretical analysis of this system with damping is significantly different from that of a simple mass spring system, and the resulting ratio of the displacement of the isolated mass to the displacement of the floor is given by

$$T = \left| \frac{1 + D\left(2\xi \frac{\omega}{\omega_n}\right)^2}{\left[1 - B\left(\frac{\omega}{\omega_n}\right)^2\right]^2 + D\left(2\xi \frac{\omega}{\omega_n}\right)^2} \right|^{\frac{1}{2}} \left[1 - \left(\frac{\omega}{\omega_n}\right)^2\right]$$

where

$$\omega_n = \sqrt{\frac{gA^2}{V_s}\left(1 + \frac{P_a}{P_g}\right)}, \text{ and}$$

ω_n is the natural frequency of the undamped system

ξ is the damping coefficient determined by the details of the damping mechanism

ω is the frequency of the vibration

B, D are constants which depend on the details of the isolator design

A is the cross sectional area of the piston

V_s is the spring chamber volume

P_g is the gauge pressure, that is the pressure in the isolator (above the pressure outside) which is dependent on the mass supported by the leg

P_a is the atmospheric pressure

Note that the transmissibility of a damped pneumatic isolator is very different from that of the damped simple harmonic oscillator of Model II, and illustrates the main features of pneumatic isolators:

1) **High performance over a wide range of loads**. The resonance frequency ω_n of the isolator is only weakly dependent upon the load M.

2) **Low natural frequency when the system is operated at several times atmospheric pressure**. In practice Newport pneumatic isolators are operated so that the air pressure in the leg is between about 40 and 80 psi.

3) **1/ω² "roll off" even with high damping and low resonance peak transmissibility**. The steep decrease in transmissibility T as the frequency increases is much faster in pneumatic isolators than the damped simple harmonic oscillator of Model II, for which the transmissibility decreases as 1/ω at high frequencies. Effectively, the damping is present only near resonance, where it is most needed.

Newport has found that the transmissibility T and resonant frequency ω_n can differ considerably from theory due primarily to effects in the design of the diaphragm and subtleties in engineering the piston and chamber design. The actual measurement of the vertical transmissibility of Newport's XL-A series leg system, is shown in Figure 1.

Designing Effective Horizontal Isolation

The pneumatic isolation described above provides isolation primarily from vertical vibrations only (actually the diaphragm alone provides some horizontal isolation). For improved, high performance

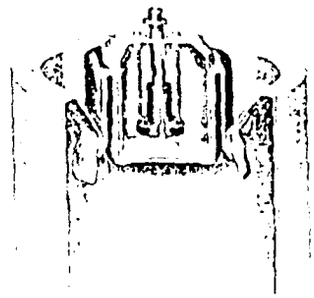

Fig 15 Newport's patented horizontal isolation system

horizontal vibration isolation another technique must be used. Newport uses a patented damped pendulum design which is schematically shown in Figure 15.

As the floor moves relative to the isolated object, the table behaves similar to a pendulum with the pivot point moving back and forth. The equations of motion thus would be the same as those of a simple harmonic oscillator, and the natural frequency of this system is:

$$f_n = \frac{\omega_n}{2\pi} = \frac{\sqrt{g/L}}{2\pi}$$

where g is the acceleration of gravity, and L is the length of the pendulum.

The actual system dynamics are more complex, and the measured natural frequency of Newport's horizontal isolation is about 1.0 Hz. For frequencies near resonance, there is amplification. However, the amount of amplification is determined by the amount of damping in the system. (Newport's XL-Series isolators have been optimally damped both vertically and horizontally.)

An important feature of Newport's patented horizontal isolation technique is that horizontal vibrations are not coupled into vertical vibrations to achieve damping, as is the case with "gimballed pistons". Actual measured transmissibility data (Figure 16) shows the horizontal isolation of the pendulum.

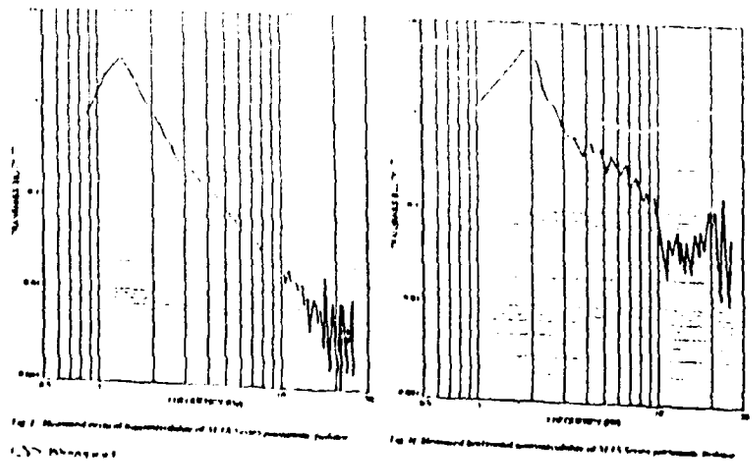

Fig 1 Measured vertical transmissibility of XL-A series pneumatic isolator

Fig 16 Measured horizontal transmissibility of XL-A series pneumatic isolator

Application of Fourier-Fresnel Imaging to Neutral - Atom Interferometry

John F. Clauser
Physics Dept., Univ. of Calif. - Berkeley
3 October, 1990

In this note we provide a brief summary of the use of of Fourier-Fresnel imaging to neutral atom interferometry. We shall see that in applications of neutral-atom interferometry not requiring the interferometer to have an open (multiply connected) topology, the use of this imaging has significant advantages, notably ease of alignment, significantly increased through-put flux, ability to work with very short wavelength (and/or high velocity atoms).

Many of the results presented here are not new, and were recognized by previous authors to have important application in electron interferometry and microscopy. Indeed, Cowley and Moodie remark that range of applications of their work to light is quite limited. The results are primarily interesting in that they span the boundary between trapezoidal Moire fringes and sinusoidal wave-interference fringes. Their limited applicability, perhaps accounts for the relative obscurity of many of the results to typical curricula of modern-day optics. The emphasis in this note is thus to put existing results (along with some additions that are needed for clarity) in a form suitable for use by techniques available for neutral-atom interferometry.

1. Possible Layouts for a Neutral-Atom Interferometer.

Figure 1. depicts two commonly discussed configurations for a neutral particle interferometer. In these, a source of neutral particles, is collimated into a narrow beam by a sequence of two slits, a distance A_c apart, each with a slit width w_c. The particles are preferably cold, slow, and possessing long deBroglie wavelength, λ. Following collimation, they pass through a sequence of three gratings (spaced respectively A_1 and A_2 apart), and thence to a detector. Since it is generally counter-productive to place significant spacing between the second collimating slit and the first grating, these elements are shown as combined into a

single finite extent grating.

The results of analyses of these configurations have frequently concluded that although the collimator may operate in the Fresnel regime ($w_c >> \sqrt{A_c \lambda}$), there is no interference visible at the third grating unless the second grating is divided into two distinct parts, with each part accepting only one fully separated diffraction order from the first grating while blocking all others; and in addition, the third grating accepts only one fully separated diffraction order from each of the parts of the second grating. Typical transmission of such a configuration is about 10^{-3}. Moreover, widening the collimator acceptance angle w_c/A_c to increase the throughput flux translates into a corresponding broadening of the diffracted beams, now causing the orders to overlap. As a result, the throughput of the collimator must also be limited with the total system throughput quite low.

An additional disadvantage of such a system is that it is difficult to align. Gratings appropriate for matter-wave deBroglie wavelengths are unsuitable for electromagnetic radiation, unless the radiation is in the soft x-ray region with a wavelength comparable to the matter-wave deBroglie wavelength.

The purpose of the present note is to indicate that, contrary to previous analyses, it is not necessary to separate the diffraction orders if the open topology is not needed for a specific application, such as one requiring exploitation of the quantum topological phase. A price one must pay for acceptance of all diffraction orders is that the input atomic beam must be more nearly monochromatic. In actuality, this price was already being paid with the separated order configurations, since use of a significantly non-monochromatic beam with them will increase each diffracted beam's angular width, and again lead to order overlap with the corresponding necessity of further reduction of w_c and consequent throughput.

2. Historical Background of Fourier-Fresnel Imaging.

In 1836 Talbot[1] reported the results of an experiment that were quite surprising. The explanation of these results was

[1] H. Talbot, Phil. Mag. 9, 401 (1836).

provided by Lord Rayleigh[2] in 1881. The reciprocal effect (with interchanged source and detector) was observed experimentally by von Lau in 1948.

A diagram of the Talbot and von Lau experimental configurations is shown in Figure 2. In the Talbot configuration, monochromatic light from a point source is focused parallel by a lens and passes through two transmission gratings (Ronchi rulings) to an extended detector. Clearly, when the gratings have zero spacing (i.e. their planes are in contact) and are oriented so that their slits are parallel, they will form a Moire pattern. As one is translated parallel to the other in its own plane in a direction perpendicular to the slits, the transmitted light intensity will vary in a periodic trapezoidal fashion (triangular when the slit width to spacing ratio is 1/2). When the gratings are separated and the translation is again performed, the trapezoidal pattern tends to wash out. Talbot's surprising result was that at grating separations that are integral multiples of a characteristic length L_T, given by

$L = n\ 2\ d^2/\lambda \equiv n\ L_{TR}$, with $n = 0, 1, 2, \ldots$ is an integer,

and d being the gratings' period, the Moire pattern reappears with high contrast. Moreover, when the integer n is odd, the pattern is trapezoidal dependence is shifted by 1/2 period.

A similar effect occurs in von Lau's configuration when an extended source is used along with a point detector at the focus of a lens following the second grating. Moreover, in von Lau's configuration, the image plane of the lens ~~between~~ displays an intensity pattern that is identical to the grating transmission function.

Since the fundamental Talbot-Rayleigh length L_{TR} is a function of the wavelength λ, the Talbot and von Lau effects clearly are examples of wave interference. Moreover, since the second grating accepts light in many diffraction orders simultaneously, a full analysis of these experiments must employ Fresnel, not Fraunhofer diffraction. Moreover, the scaling of L_{TR} is intriguing for neutral atom interferometry, since it has convenient values when calculated in terms of available atomic

[2]Lord Rayleigh, Phil. Mag. 11, 196 (1881).

deBroglie wavelengths and micro-fabricated gratings. However, neither the Talbot nor von Lau configurations are directly suitable for matter - wave interferometry because of the required presence of a lens.

Cowley and Moodie[3] provided a theoretical and experimental analysis in 1957 of the images of a point source formed by a transmission grating. They found that when a condition on the geometry is satisfied (similar to the Talbot-Rayleigh condition given above), the image plane of the grating displays an intensity pattern that is a magnified exact replica of the imaging grating. When the point source is replaced by a grating in their analysis, they produce an intermediate configuration which contains the Talbot and von Lau configurations as limiting cases (source and/or detector moved to infinity). Note that these configurations do not involve the use of a lens, and as such are eminently suitable for use in matter-wave interferometry (an application of their results that they noted).

Winthrop and Worthington[4] reanalyzed the Cowley and Moodie configuration in 1965 and discovered the existence of additional high contrast images that do not satisfy the Talbot-Rayleigh condition, and do not provide exact replicas of the imaging grating. They called these additional images Fresnel images, reserving the term Fourier images for those that form exact magnified images. Fresnel images of an intensity distribution that consists of a multiplicity of magnified replicas (aliases) of the original grating.

3. Application of Fourier - Fresnel imaging to neutral - atom Interferometry

We now summarize and apply the above results to a configuration suitable for matter-wave interferometry. Consider a sequence of three broad transmission gratings, whose planes are spaced a distance R apart. The middle grating has equally spaced open (vacuum) slits of width s with periodic spacing d, while the

[3] J.M.Cowley and A.F.Moodie, Proc. Phys. Soc. (London) 70, 486,497,505 (1957).

[4] J.T.Winthrop and C.R.Worthington, JOSA, 55, 373 (1965).

first an third gratings have open slits of width 2s with periodic spacing 2d. A convenient ratio of s/d = 0.1 will suffice for our purposes, but this choice is not critical. The sequence is diffusely illuminated by nearly monochromatic but weakly collimated neutral-atom deBroglie waves. In this configuration, unlike the configurations discussed earlier for neutral atom interferometers, the middle grating is not split into two parts.

Let us define a characteristic wavelength for this configuration $\lambda_{TR} \equiv d^2 / R$. The first grating forms a series of small equally spaced incoherent sources, each one illuminating the second grating. All possible Fresnel diffraction orders of the second grating then reach the third grating. Following the above results, when the atomic debroglie wavelength $\lambda = \frac{n}{n} \lambda_{TR}$ then each source point on the first grating will form an image on the third grating consisting of a series of n stripes per 2d, each of width s. (When n = 1 holds, the images are Fourier images. When n > 1 holds the images are Fresnel images, by Winthrop and Worthington's definition.) If every n'th stripe is positioned on an open slit of the third grating, then transmission will occur. If the third grating is slowly translated across its own pattern, then the transmission will vary periodically with spatial period of 2d/n. When λ / λ_{TR} is not a ratio of two small integers, periodic transmission does not occur. The pericdic transmission signal can then easily be measured using standard phase sensitive detection (lock-in) techniques.

Since each source point of the first grating provides exactly the same pattern, the periodic set of sources provided by the first grating will increase the intensity transmitted by the third grating in proportion to the number of sources. Correspondingly, since the sizes of the second and third gratings may be increased without limit, a very high detector flux will thus be obtained.

An additional interesting effect can be observed when one varies λ. Transmission resonances can be observed when $\lambda \approx \lambda_{TR} m/n$ holds. If one monitors the aforementioned periodic transmission at the n-th harmonic, there will occur a resonance whenever m is approximately integral. The width and shape of these resonances

(Resonances with both m and n odd are opposite phase.)

depends on (s/d), m and n. When the atomic beam has a dominantly particle-like character (as opposed to wave-like) the n = 1 resonance reappears. Thus, in the high velocity limit (i.e. beam cooler/decelerator turned off), the three gratings form only geometric shadows, and a simple Moire pattern results. This wave-particle transition occurs when the deBroglie wavelength is sufficiently short that any point on the third grating is illuminated by at most one slit.

The above configuration will also work as a sensitive inertial sensor, in the same sense as the earlier considered interferometers. The path from any source point to any image point forms a set of nested diamond shape interferometers, each with its own inertial sensing capability. However, each such interferometer has a different area. Thus if significant gravitational or Coriolis force is applied to the atoms, the various interferometers within the nest will get out of phase and the interference will disappear. Thus the magnetic-field servo system discussed earlier by the author can be used to keep the atoms sensing essentially the equivalent of an inertial frame, and the inertial signals obtained from the servo system error signal.

Finally, let us discuss a further advantage of the system thus described. That is its ease of alignment. It was noted above that in the high velocity limit (i.e. beam cooler/decelerator turned off), the gratings form only geometric shadows, and a simple Moire pattern results. Using the same phase sensitive detection technique, one then can align the gratings to this Moire pattern by maximizing the n = 1 harmonic signal. In addition, since the grating period d can be much larger than that required for the separated beam configurations, these gratings can now be incorporated as elements of an *in-situ* optical interferometer, and the coarse alignment performed with light.

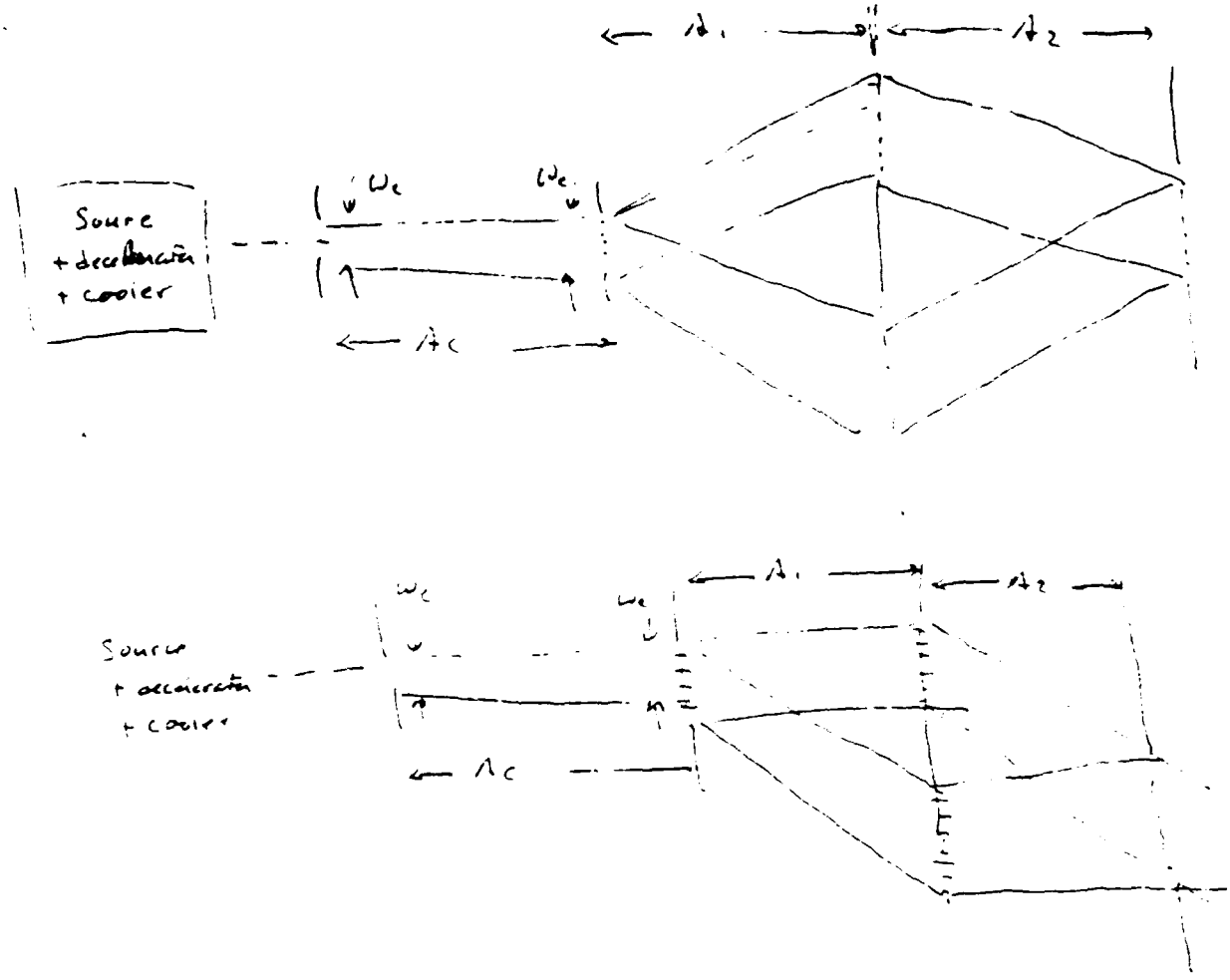

Fig 1 Configurations in Separated beam matter-wave interferometry

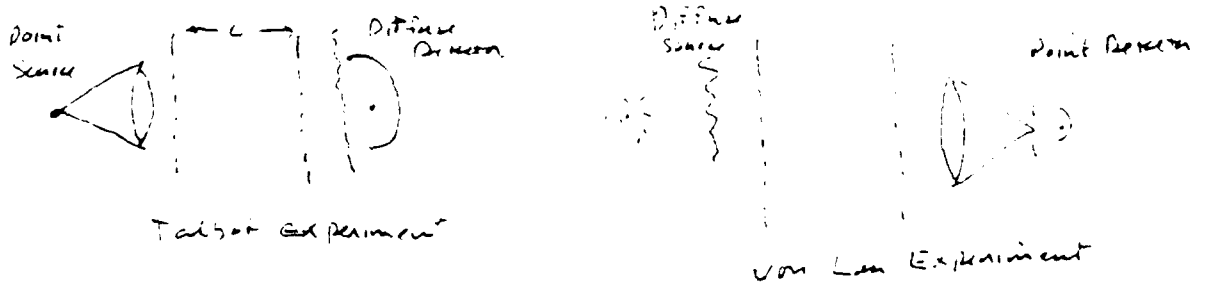

Talbot experiment

Von Laue Experiment

Fig 2

10/5/90

Response to Summary Questionnaire

To: Hersch Pilloff
Physics Divn. (Code 1112LO)
Office of Naval Research
800 North Quincy Street
Arlington, VA 22217 - 5000

Re: R&T 4124123

From: John F. Clauser - P.I.
Dept. of Physics
University of California
Berkeley, CA 94720

Project: Neutral-Atom Matter-Wave Interferometry

Grant #: N00014-90-J-1475

1.Research Description:

The research program is to study the spatial wave-like character of freely propagating neutral-atom matter-waves (deBroglie waves). To do so, we are constructing and using a neutral-atom matter-wave interferometer. An atomic beam will be decelerated and cooled by conventional laser spontaneous cooling. It will be extracted from the laser cooling apparatus and fed through a series of micro-fabricated transmission gratings, which will serve as an interferometer, and thence to a detector.

2.Scientific Problem:

Matter-wave interferometry has here-to-fore been been performed with photons, electrons, neutrons, and Cooper electron pairs. Can this list be extended to include neutral atoms? What are the fundamental issues and constraints in doing so? Although the framework of quantum mechanics appears eminently successful in describing the micro domain of nature's building blocks, it is troubled by conceptual problems and counter-intuitive (or at the very least, surprising) predictions when it is applied to the macroscopic domain. Thus, its applicability within the macroscopic domain is frequently questioned and/or poorly understood. The experiments being performed will attempt to answer the above two questions, as well as to track the evolution of quantum systems in

the macro domain, in a parameter range that spans their classical particle-like behavior through their quantum wave-like behavior.

The research is also useful in providing a new form of scientific instrumentation. If indeed a neutral-atom interferometer can be built, then a wide variety of fundamental problems become experimentally accessible. In atomic physics one will be able to measure complex atomic scattering amplitudes and measure spin-independent energy level shifts. In geodesy and geophysics and navigation, ultra sensitive measurements of gravity, gravity gradients, rotation and acceleration will become available. A whole host of effects predicted by relativistic gravitational theory may become measurable. Finally, many predicted quantum topological effects and other counter-intuitive quantum mechanical effects in the macroscopic domain become measurable.

3.Scientific and Technical Approach:

The essence of our approach is outlined under Research Description, above. The apparatus consists of a three meter tall, vertical orientation, stainless steel, ultra-high vacuum chamber. It is mounted on a gimbaled vibration isolating framework. The lowest portion contains an atomic beam oven. Light from a diode laser is reflected off a 45° mirror with a slit in it, so as to counter-propagate along the atomic beam exiting the oven. The laser is amplitude modulated at an atomic hyperfine resonance and wavelength-chirped at a kiloHertz sawtooth rate. A decelerated, cooled neutral potassium beam should the emerge from the mirror's slit.

The cooled beam then propagates upward through a sequence of three micro-fabricated gratings. Grating positions can be manipulated through bellows seals. At each grating the beam undergoes wave-like diffraction and is thereby dispersed. The gratings are arranged to allow recombination of the dispersed waves so as to interfere and form a macroscopic standing matter-wave at the surface of the third grating. Upon transmission by the third grating, a Moiré pattern is formed. The transmitted

beam flux is monitored by a hot-wire detector. Upon manipulation of externally imposed fields (gravitational, Coriolis, magnetic, and/or electric)upon the matter-waves within the interferometer, and/or manipulation of the grating positions, the standing wave pattern may be detected and measured, via the resulting variation of the transmitted atomic flux.

4a.Progress:

As of this writing, the ONR Grant has been in force for only eight months. During this period, two graduate students have been brought on to the project. The chamber was reassembled and brought to full high-vacuum operation. A new beam oven was fabricated and installed. A thermal potassium beam was produced and detected. Initial testing and various improvements to the vibration isolation mounting have proceeded. Various laser diodes have been operated and temperature tuned. Construction of a cooled Littrow grating Fabry Perot laser cavity has proceeded and nears completion and testing. A study of Fourier-Fresnel imaging (also called Talbot-fringe detection) introduced by the author at an ONR sponsored Matter-Wave Interferometry Workshop, Jan.1990 in Santa Fe, has continued. Results of the study indicate that the use of these techniques provides many advantages. Their use will be incorporated into the initial experiments. Possible sources for matter-wave gratings have been evaluated and it has been concluded that the most expeditious, cost effective, and convenient source is to build them ourselves at the Univ. of Calif. - Berkeley Cory Hall facility. The construction of a laser fluorescence monitor for beam velocity monitoring is approaching completion and testing.

4b.Special Significance of Results:

See Fourier-Fresnel imaging (4a, above).

5. Extenuating Circumstances:

See 8, below.

6.Publications:

None.

7.Unspent Funds:

None anticipated.

8.Other Support:

One graduate student, Mathias Rench, is supported on a Dept. of Education Fellowship.

The project had been underway for several years prior to the commencement of the ONR grant. During this time it was solely supported by the personal funds of John F. Clauser, (who, as such, retains sole title to patents accruing to this earlier work - see copy of letter from John F. Clauser to Univ. of Calif. Regents discussing such patent applications, a copy of which was included as an Appendix to the Grant Proposal).

The present ONR Grant provides insufficient funding for the performance of the project, which, as a result, is funded jointly by the personal funds of John F. Clauser. Since the grant has been in force, other than personnel costs and associated University of Calif. overhead, all expenses, including those for equipment, supplies, travel, computers, office work and incidentals have been paid for personally by John F. Clauser.

9.Major Equipment Purchases:

None